Research Article | Vol. 10, No. 8 | 1 Aug 2019 | BIOMEDICAL OPTICS EXPRESS 3929
Biomedical Optics EXPRESS

Optofluidic microcapillary biosensor for label-free, low glucose concentration detection

HONGDAN WAN,[1,3] JIJING CHEN,[1] CHENG WAN,[2] QUAN ZHOU,[1] JIE WANG,[1] AND ZUXING ZHANG[1,4]

[1]*Nanjing University of Posts and Telecommunications, Nanjing 210023, China*
[2]*Department of Biomedical Engineering, College of Engineering of Peking University, Beijing, China*
[3]*hdwan@njupt.edu.cn*
[4]*zxzhang@njupt.edu.cn*

Abstract: We demonstrate label-free detection of low glucose concentration based on whispery gallery mode resonance in an optofluidic microcapillary (OFMC) biosensor. The wall surface of the OFMC is bio-chemically functionalized to detect cellular-level glucose concentration as low as 2.78 mM. The measured sensitivity is 0.966 pm/mM. The fabricated microcapillary has a thin wall thickness of 2 μm and a Q factor of 1.3×10^6, corresponding to a bulk refractive index sensitivity of 23.36 nm/RIU. The OFMC biosensor has advantages such as high resistance to environmental perturbation, small sample volume down to 90 nL and cost-effectiveness. Theoretical analysis shows the sensor sensitivity depends on the microcapillary wall thickness and liquid core refractive index.

1. Introduction

Glucose is an important bioactive substance in human blood for energy supply and metabolism. For diabetic patients, an intracellular glucose level of human blood lower than 3.9 mM can lead to fainting, coma, and even death [1]. Till date, various methods for glucose detection are proposed, however, low glucose concentration detection is still important.

Previously, electrochemical biosensors are applied [2]. Y. H. Song et.al. proposed a glucose biosensor based on the 3D-KSC/NCNTs/GOD electrode [3]. However, due to its complicated operating procedures, non-portability and difficulties in obtaining enough signal transduction, it does not meet clinical demands [4]. In recent years, biosensors manufactured from optical fiber are proposed to detect concentrations of various aqueous solutions due to their advantages of high efficiency, low cost, and accurate measurement [5]. Enhanced optical detection of D-glucose with a concentration detection limit of 1 nM was achieved by Sridevi S. et al., using the etched fiber Bragg gratings coated with aminophenylboronic acid (APBA)-functionalized reduced graphene oxide [4]. B. B. Luo reported an excessively tilted fiber grating (Ex-TFG) inscribed in the thin-cladding optical fiber (TCOF) serve as label free and selective glucose sensor with the sensitivity of 1.514 nm/(mg/ml) [6]. Y. Q. Yuan et al. demonstrated a terminal reflection fiber surface plasmon resonance (SPR) sensor with a sensitivity of 2.52 nm/mM [7]. A highly sensitive glucose detection refractometer based on Mach-Zehnder Interferometer (MZI) is proposed by V. Bhardwaj et al. with the sensitivity of 380 nm/RIU [8]. A label-free MZI optical biosensor with a bulk refractive index detection sensitivity of 84,000 rad/RIU/cm was also reported by S. R. Hu, et al [9]. They also demonstrated a planar silicon photonic biosensor with high detection sensitivity and a short response time through increased probe molecule density [10]. However, for most of the single-pass optical fiber biosensors, light interacts with the sensing target solution only once. One must increase the physical length of the sensor, thus need more sample solution to enhance the interaction between them. In a resonator-based sensor where light is confined in the form of whispery gallery mode (WGM) in a micron-scale, the light waves interfere constructively, the effective interaction length can be increased by increasing the optical

#366821 https://doi.org/10.1364/BOE.10.003929
Journal © 2019 Received 8 May 2019; revised 29 Jun 2019; accepted 2 Jul 2019; published 12 Jul 2019

Biomedical Optics EXPRESS

quality factor (Q) of the resonator [11]. In recent years, sensitive and label-free detection of biomolecules such as viruses, DNA and proteins are implemented by various WGM resonator biosensors. WGM will change when it reactively interacts with a bound small protein molecule on the surface of a silica microsphere resonator [12].

A slightly deformed microcavity is employed to monitor the mode broadening caused by transferring 70 nm-radius polystyrene (PS) particles to surface of the microcavity [13]. Different from solid-core WGM resonators, hollow-core microcavities can act as fluidic input/output channels, which can handle aqueous solutions of small volume. The unique capability of integrating with microfluidics and excellent optical confinement of their WGMs make hollow-core microcavities one of the most promising optofluidic platforms for sensitive chemical and biosensing of aqueous solutions [14].

In this paper, we propose and demonstrate an optofluidic biosensor based on a thin wall microcapillary resonator for label free, low concentration glucose detection. To the best of our knowledge, this is the first report on detecting glucose concentration as low as 2.78 mM based on a bio-mechanically functionalized optofluidic microcapillary (OFMC) with high Q and small sample volume. Sensing performance of the biosensor is analyzed both theoretically and experimentally.

2. Sensor fabrication and experimental setup

2.1 Modeling and simulation

As shown in Fig. 1(a), FDTD method is used to simulate the WGM spectra of the OFMC with different liquid core refractive indices (RIs). The simulation parameters are as follows: The light source is transverse-electric (TE) polarized with wavelength swept from 1.5 to 1.6 μm. The simulation grid size is 100 nm and the resulting spectral resolution is 0.002 nm. The material refractive indices of the taper and the microcapillary are 1.4446. The waist diameter of the fiber taper is 1 μm, the wall thickness and the outer diameter of the microcapillary are 0.8 μm and 10 μm, respectively. The diameters chosen in the simulation are significantly smaller than those in the experiment. The coupling distance between the fiber taper and the microcapillary is set to 400 nm. Figure 1(b) shows the wavelength shift of the WGM spectra as a function of the liquid core RI. The simulation results show a linear slope of 27.3 nm/RIU over the RI range from 1.34 to 1.42.

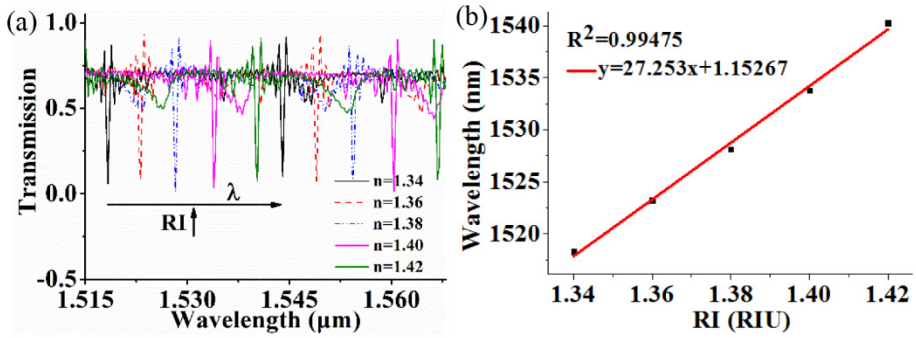

Fig. 1. (a) Simulated WGM spectra of the OFMC with different liquid core RIs, (b) Wavelength shift of the WGM spectra with different liquid core RIs.

Then, sensitivity of the OFMC with different wall thicknesses is also investigated. The outer diameter of the microcapillary is about 50 μm. The wall thicknesses are 1 μm, 2 μm, 3μm and 4 μm. Use m, l to represent the natural axial mode number and an azimuthal mode number, respectively [16]. The modal intensity distributions of the WGM (m = 1, l = 338) with different wall thicknesses are simulated and compared in Fig. 2. It can be seen clearly

Biomedical Optics EXPRESS

that the modal intensity distribution of the WGM in the microcapillary resonator shifts into the inner wall as the wall thickness decreases, which can enhance the sensing ability.

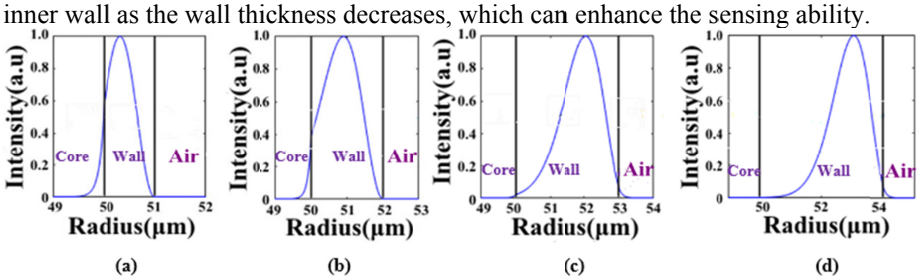

Fig. 2. Numerical simulation of the WGM modal (m = 1, l = 338) intensity distributions of the OFMC with four wall thicknesses: (a) 1 μm; (b) 2 μm; (c) 3 μm; (d) 4 μm.

Figure 3 shows the numerical simulation of the RI sensitivity of the OFMC as a function of the wall thickness. It can be seen that the sensitivity decreases with an increased wall thickness from 1 μm to 4 μm. For a wall thickness> 3 μm, the sensor is disabled.

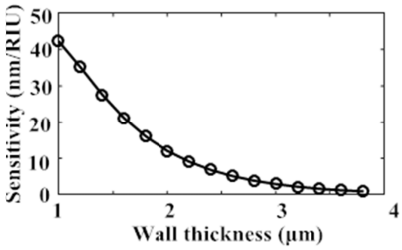

Fig. 3. Sensitivity versus the wall thickness.

2.2 Sensor fabrication and experimental setups

Figure 4 shows the microscopic image of the fiber taper-coupled microcapillary resonator. The inflation and tapering method are used to fabricate the thin-wall microcapillary with an outer diameter of 86.8 μm and a wall thickness of 2.2 μm, observed by a high-resolution vertical microscope system consisting of a 500-magapixel charge-coupled-device (CCD) camera. The WGM was excited in the microcapillary resonator using the tapered fiber and the Q factor of the microcapillary we fabricated is measured to be about 1.3×10^6. The gap between the microcapillary and the fiber taper (with a waist diameter of about 2-3 μm) is controlled by electromechanical 3D stages with 20 nm resolution. Over coupling is used to ensure the sensor stability. There several reasons for selecting microcapillary as the WGM resonator: the advantage of combining the WGM properties with the intrinsic capability of integrated microfluidics [17], the Q-factor is relatively higher, the tubing wall of a microcapillary is thin and curved and has a large surface area [15]. All of which are helpful for effectively exciting a strong evanescent field over a short distance and benefit for achieving small sample volume and sensitive glucose detection.

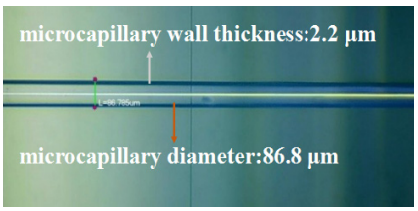

Fig. 4. Microscope image of the fiber taper-coupled microcapillary resonator.

Biomedical Optics EXPRESS

The experimental setup of the proposed OFMC biosensor is shown in Fig. 5. Aqueous solutions are flowed through the microcapillary by a syringe pump with a minimum speed resolution of ~0.1 μm and a minimum flow rate of ~7 μL/min. A tunable laser source (TLS) with a narrow linewidth of 5 kHz and a wavelength tuning range of 90 nm near 1550 nm is pump into the fiber taper and excites the WGM. The WGM spectra are recorded by a photodetector (PD, New Focus 1811) with a bandwidth of 125 MHz. The polarization controller (PC) controls the polarization state of the incident light for optimal coupling condition.

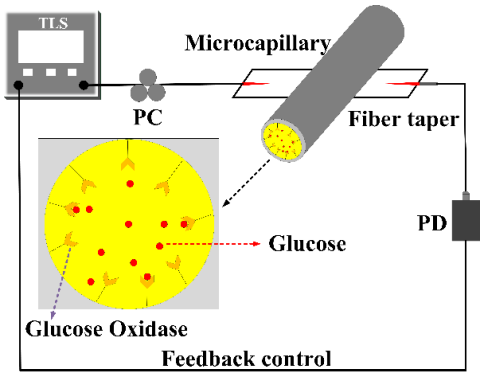

Fig. 5. Schematic diagram of the experimental setup of the OFMC biosensor.

2.4 Sensor calibration

Firstly, deionized water is flowed into the microcapillary to test sensor stability with aqueous solution injected. The WGM spectra of the OFMC are recorded every 10 minutes and measured for 1 hour, as shown in Fig. 6. The maximum wavelength fluctuation of the WGM spectrum is about 0.89 pm. WGM resonance in the OFMC is not only sensitive to target analyte but also sensitive to environmental disturbances such as mechanical vibration and temperature change. For a detectable target analyte variation, the wavelength shift of the WGM spectrum should be larger than 0.89 pm. The proposed sensor system is placed on a vibration isolation platform, thus temperature perturbation is the most harmful noise sources and further improvements should be considered to suppress the sensor instability.

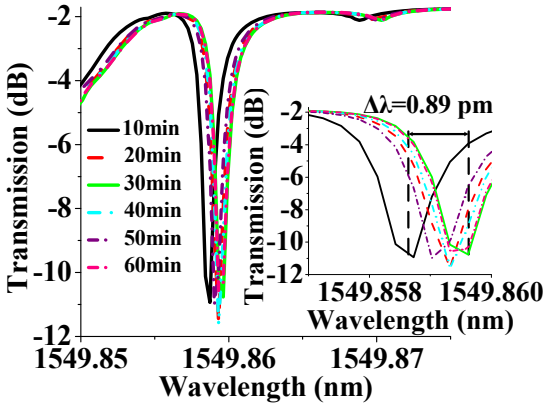

Fig. 6. WGM spectra of the OFMC measured within 1 hour. Insets: Zoom-in-view of the wavelength shift of the WGM spectra.

Then, we flow aqueous NaCl solutions with five different concentrations into the OFMC. The RI of each solution is measured with an Abbe refractometer for five times, as shown in Table 1.

Biomedical Optics EXPRESS

Table 1. RIs of the NaCl Solution with Five Different Concentrations and Each Measured for 5 times.

Concentration	1st	2nd	3rd	4th	5th	Average RI
2.6%	1.3375	1.3374	1.3374	1.3374	1.3373	1.3374
2.8%	1.3375	1.3376	1.3376	1.3378	1.3376	1.3376
3.0%	1.3380	1.3381	1.3382	1.3381	1.3382	1.3381
3.2%	1.3384	1.3384	1.3385	1.3385	1.3384	1.3384
3.4%	1.3390	1.3388	1.3389	1.3386	1.3388	1.3388

Then, we kept the fiber taper-microcapillary coupling condition stable and unchanged. The NaCl solutions with increased concentration are flowed into the microcapillary resonator. The measured WGM spectra of the OFMC are compared in Fig. 7. It can be seen that the WGM spectra is red-shifted for an increased NaCl concentration flowed through the resonator, thus an increased RI of the aqueous solution results in longer WGM resonance wavelength.

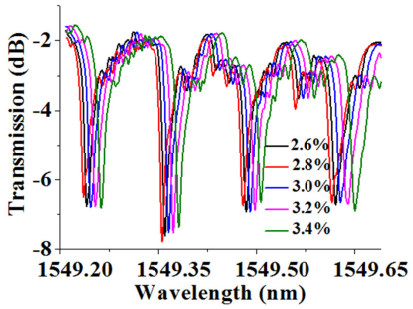

Fig. 7. WGM spectra shift to longer wavelength when the NaCl solutions with increased concentration are flowed into the OFMC.

Figure 8 shows the measured WGM wavelength shift as a function of the RI change of the NaCl solution due to different concentrations. The bulk refractive index sensitivity (BRIS) of the OFMC is calculated to be 23.36 nm/RIU.

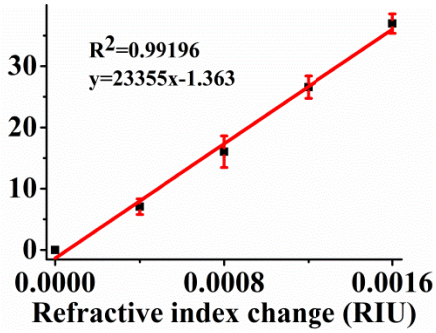

Fig. 8. Measured BRIS of the OFMC.

2.3 Surface bio-chemical functionalization

Low glucose concentration detection is performed based on the experimental setup as shown in Fig. 5. Deionized water is firstly flowed into the OFMC without functionalization, being referenced as the initial experimental condition with a glucose concentration of 0 mM. Then, six groups of glucose solutions with concentrations varied from 2.78 mM to 16.67 mM are prepared and flowed into the unfunctionalized OFMC sequentially with the sample volume of

Biomedical Optics EXPRESS

about 90 nL, having an ascending concentration for detection. When solution concentration is 2.78 mM, the amount of glucose molecules inside is about 2.5×10^{-7} mmol, the refractive index change of the low concentration glucose solution is $\sim 10^{-3}$, correspond to an undetectable WGM wavelength shift of < 0.89 pm. Figure 9 shows the WGM wavelength shift from glucose concentration of 0 mM to 16.67 mM. It can be seen that using the unfunctionalized microcapillary for detection, the maximum concentration difference of 13.89 mM results in a small wavelength shift of about 2.63 pm.

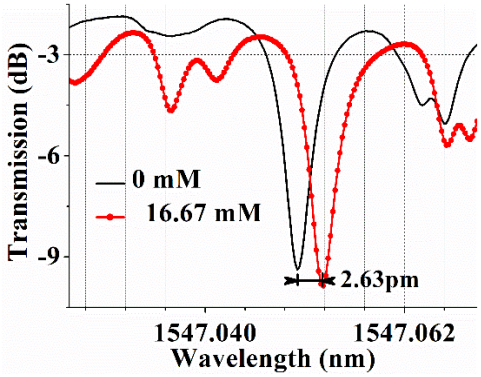

Fig. 9. WGM spectra of the unfunctionalized OFMC with glucose concentration of 0 mM and 16.67 mM. The wavelength is red-shifted with 2.63 pm.

The cross-link of the analyte and the inner wall surface of the hollow resonator can be considered as the first-order perturbation of light propagation when microfluidic technology is combined with a fiber taper-coupled microcapillary, the change of the propagation constant can be calculated as [15]:

$$\frac{\delta(\Delta\beta)_b}{\Delta\beta} = \frac{\tau\alpha_{ex}\sigma_P \int \left|\mathrm{E(x,y)}^2 dL\right|}{2\varepsilon_s \iint \left|\mathrm{E(x,y)}^2\right| dxdy} \tag{1}$$

Where, σ_p is the biomolecular surface density, ε_s is the relative permittivity, α_{ex} represents the excess polarization due to a single biomolecule, τ denotes the change of field intensity near the inner wall surface after surface functionalization, the magnitude of which is related to the refractive index and the thickness of the layer. The integral of the denominator represents the mode energy over the entire waveguide cross section. Since most of the energy is confined in the microcapillary wall, the integrated amplitudes of the two modes (fiber mode and hybrid mode) are almost the same. The integration of the numerator illustrates the energy density of the inner wall surface of the microcapillary. After differentiating (1), we can get:

$$\Delta\lambda = \frac{d(\Delta\beta)}{\frac{\delta(\Delta\beta)}{\delta\lambda}} \tag{2}$$

Equation (2) illustrates the transduction mechanism from evanescently induced change of $\Delta\beta$ into the detectable wavelength shift. Capturing more glucose molecules on the microcapillary wall can cause larger refractive index change and enhance the wavelength shift. Surface bio-chemical functionalization of the microcapillary is thus performed for enhancing the wavelength shift caused by variation of the glucose concentration.

The inner wall surface of the microcapillary is functionalized with glucose oxidase (GOD) to capture more glucose molecules. The bio-chemical reagents required for surface functionalization are: deionized water, sodium acetate reagent, absolute ethanol, anhydrous glucose, GOD, nitric acid, concentrated sulfuric acid, and hydrogen peroxide. The surface

Biomedical Optics EXPRESS

functionalization steps are as follows: Firstly, deionized water is introduced into the microcapillary for several times to ensure that the microcapillary is clean. Then, a dilute nitric acid with a concentration of 5% is injected and sealed in the microcapillary, standing for 2.5 hours (Step I). Secondly, the microcapillary is cleaned alternately by deionized water and alcohol. Then, the concentrated H_2SO_4 aqueous solution of hydrogen peroxide (95% by volume of concentrated sulfuric acid) is injected and sealed in the microcapillary for 1 hour to ensure that the hydroxyl group on the inner wall surface of the OFMC is fully activated (Step II). Next, the microcapillary is kept hollow and dried at room temperature. The 3-aminopropyltriethoxysilane (APTES) solution is pumped into the microcapillary after drying, and then the OFMC is let stand for 30 minutes, rinsed with deionized water and alcohol to remove non-covalently bonded silane compounds in the chamber (Step III). Then, a 10 mg/ml glucose oxidase (GOD) solution (solvent is a sodium acetate buffer solution) is injected into the microcapillary. The solution is let stand for 2 hours to ensure that the GOD-COOH group sufficiently reacted with the NH_3^+ after salinization on the inner surface of the microcapillary (Step IV). Finally, the inside of the microcapillary is rinsed successively with sodium acetate buffer solution and deionized water, and then let dry (Step V). The surface functionalization of the OFMC is thus completed.

3. Results and discussions

It is important that during the surface functionalization process, the coupling of the microcapillary and the fiber taper is kept stable. After surface functionalization of the inner wall of the microcapillary, the glucose solution is measured with the same procedure as the unfunctionalized one. As shown in Fig. 10, the measured WGM spectra is red-shifted to a longer wavelength as the concentration of the glucose solution increases. It can be seen clearly from the zoom-in-view of Fig. 10, the wavelength shift caused by low glucose concentration variation of 2.78 mM is now detectable, which is about 2.71 pm. The WGM resonance wavelength for the glucose concentration of 0 mM is shifted from 1547.12211 nm to 1547.13865 nm for the glucose concentration of 16.67 mM. The spectral shift range reaches 16.54 pm, which is more than 6 times larger than the unfunctionalized one with the same glucose concentration variation.

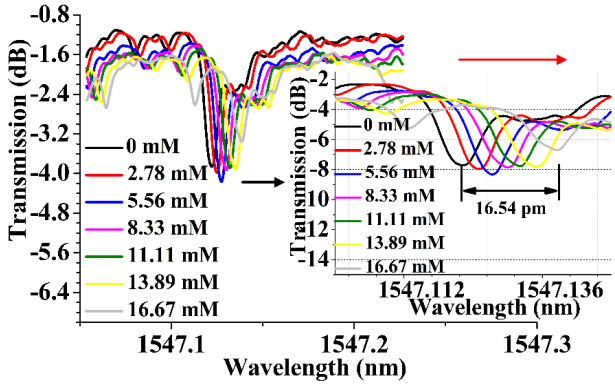

Fig. 10. Measured WGM spectra of the OFMC flowing through glucose solution with an increased concentration and the zoom-in-view of the red-shift WGM spectra.

The experimental results confirmed that, the glucose detection sensitivity of the OFMC is greatly improved after the surface bio-chemical functionalization. Figure 11 shows the linear fitting results of the wavelength shift as a function of the glucose concentration. The sensitivity of the functionalized OFMC is about 0.966 pm/mM.

Biomedical Optics EXPRESS

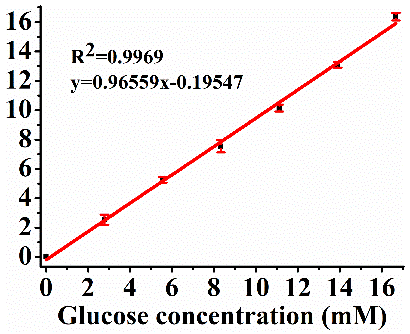

Fig. 11. Linear fitting of the glucose detection sensitivity.

4. Conclusions

In conclusion, we demonstrate an OFMC biosensor for label free, low concentration glucose detection. Surface functionalization is used to enhance the sensitivity of the OFMC. The detection sensitivity of 0.966 pm/mM is achieved by our fabricated OFMC with a Q factor of 1.3×10^6. The minimum detectable glucose concentration is 2.78 mM, with a small sample volume down to 90 nL. The simulation results depict the sensitivity is dependent on microcapillary wall thickness and refractive index significantly. This OFMC biosensor will have potential in biomedical and chemical sensing applications due to its merits of high stability, fast detection as well as high cost-effectiveness. The detection capability was analyzed both theoretically and experimentally.

Funding

National Natural Science Foundation of China (11704199); Natural Science Foundation of Jiangsu Province (BK20161521); Postgraduate Research & Practice Innovation Program of Jiangsu Province (SJKY19_0815); the STITP of NUPT.

Disclosures

The authors declare there are no conflicts of interest.

References

1. D. J. Macaya, M. Nikolou, S. Takamatsua, J. T. Mabeck, R. M. Owens, and G. G. Malliaras, "Simple glucose sensors with micromolar sensitivity based on organic electrochemical transistors," Sens. Actuators B Chem. **123**(1), 374–378 (2007).
2. R. Devasenathipathy, V. Mani, S. M. Chen, S. T. Huang, T. T. Huang, C. M. Lin, K. Y. Hwa, T. Y. Chen, and B. J. Chen, "Glucose biosensor based on glucose oxidase immobilized at gold nanoparticles decorated graphene-carbon nanotubes," Enzyme Microb. Technol. **78**, 40–45 (2015).
3. Y. Song, X. Lu, Y. Li, Q. Guo, S. Chen, L. Mao, H. Hou, and L. Wang, "Nitrogen-doped carbon nanotubes supported by macroporous carbon as an efficient enzymatic biosensing platform for glucose," Anal. Chem. **88**(2), 1371–1377 (2016).
4. S. Sridevi, K. S. Vasu, S. Sampath, S. Asokan, and A. K. Sood, "Optical detection of glucose and glycated hemoglobin using etched fiber Bragg gratings coated with functionalized reduced graphene oxide," J. Biophotonics **9**(7), 760–769 (2016).
5. A. Leunga, P. M. Shankar, and R. Mutharasan, "A review of fiber-optic biosensors," Sens. Actuators B Chem. **125**(2), 688–703 (2007).
6. B. Luo, Z. Yan, Z. Sun, Y. Liu, M. Zhao, and L. Zhang, "Biosensor based on excessively tilted fiber grating in thin-cladding optical fiber for sensitive and selective detection of low glucose concentration," Opt. Express **23**(25), 32429–32440 (2015).
7. Y. Yuan, X. Yang, D. Gong, F. Liu, W. Hu, W. Cai, J. Huang, and M. Yang, "Investigation for terminal reflection optical fiber SPR glucose sensor and glucose sensitive membrane with immobilized GODs," Opt. Express **25**(4), 3884–3898 (2017).
8. V. Bhardwaj and V. K. Singh, "Fabrication and characterization of cascaded tapered Mach-Zehnder interferometer for refractive index sensing," Sens. Actuators A Phys. **244**, 30–34 (2016).
9. K. Qin, S. Hu, S. T. Retterer, I. I. Kravchenko, and S. M. Weiss, "Slow light Mach-Zehnder interferometer as label-free biosensor with scalable sensitivity," Opt. Lett. **41**(4), 753–756 (2016).

Biomedical Optics EXPRESS

10. S. R. Hu, Y. L. Zhao, K. Qin, S. T. Retterer, I. I. Kravchenko, and S. M. Weiss, "Enhancing the sensitivity of label-free silicon photonic biosensors through increased probe molecule density," ACS Photonics **1**(7), 590–597 (2014).
11. F. Vollmer and L. Yang, "Label-free detection with high-Q microcavities: a review of biosensing mechanisms for integrated devices," Nanophotonics **1**(3-4), 267–291 (2012).
12. F. Vollmer and S. Arnold, "Whispering-gallery-mode biosensing: label-free detection down to single molecules," Nat. Methods **5**(7), 591–596 (2008).
13. L. Shao, X. F. Jiang, X. C. Yu, B. B. Li, W. R. Clements, F. Vollmer, W. Wang, Y. F. Xiao, and Q. Gong, "Detection of single nanoparticles and lentiviruses using microcavity resonance broadening," Adv. Mater. **25**(39), 5616–5620 (2013).
14. T. Tang, X. Wu, L. Liu, and L. Xu, "Packaged optofluidic microbubble resonators for optical sensing," Appl. Opt. **55**(2), 395–399 (2016).
15. L. L. Liang, L. Jin, Y. Ran, L. P. Sun, and B. O. Guan, "Interferometric detection of microRNAs using a capillary optofluidic sensor," Sens. Actuators B Chem. **242**, 999–1006 (2017).
16. H. Zhu, I. M. White, J. D. Suter, P. S. Dale, and X. Fan, "Analysis of biomolecule detection with optofluidic ring resonator sensors," Opt. Express **15**(15), 9139–9146 (2007).
17. A. Giannetti, B. S. Berneschi, A. Cosci, F. Cosi, and D. Farnesi, "Optical micro-bubble resonators as promising biosensors," Opt. Sensors. International Society for Optics and Photonics, (2015).